

# AN EVALUATION OF THE PERMEABILITY OF A JEWELRY CASTING INVESTMENT

**John C. McCloskey, David Allen, and Alfred Thibodeaux  
Stuller Settings, Inc., Lafayette, Louisiana**

## **Abstract**

The permeability of gypsum bonded silica jewelry investment was measured at the elevated temperatures that are typically used in jewelry investment casting operations. Measurements were performed on samples with cylindrical geometries that were similar to the geometry of investment casting molds. A unique method for measuring mold cavity pressures, temperatures, and flow rate of air through mold walls was developed and utilized.

## **Key words**

Investment casting, gypsum bonded silica investment, D'Arcy's Law, vacuum assisted casting, permeability, flow-pressure measurement.

## **An Evaluation of the Permeability of a Jewelry Casting Investment**

**John C. McCloskey, David Allen, and Alfred Thibodeaux**  
**Stuller Settings, Inc., Lafayette, Louisiana**

A comprehensive explanation of the permeability characteristics of silica based, gypsum bonded jewelry casting investments is not readily available in the technical literature of jewelry manufacturing. Scharwartz<sup>1</sup>, and Kingery<sup>2</sup> describe the "setting process", or the rehydration of calcined gypsum, that can be applied to silica-gypsum casting investments. Ott<sup>3</sup> describes some techniques that have been used to evaluate the permeability characteristics of gypsum bonded investment. These references have been used as starting points for developing a physical model for jewelry investment and evaluating methods for measuring investment permeability characteristics at elevated temperatures.

### **THE STRUCTURE OF JEWELRY INVESTMENT.**

Jewelry investment is a blend of fine silica particles and calcined gypsum. Schwartz<sup>1</sup> and Kingery<sup>2</sup> describe how the calcined gypsum phase dissolves and reprecipitates when mixed with water to form a felt-like structure of very fine needles. This suggests that when a jewelry investment is mixed with water and processed through a typical burnout cycle, the resulting structure contains silica particles embedded in a porous

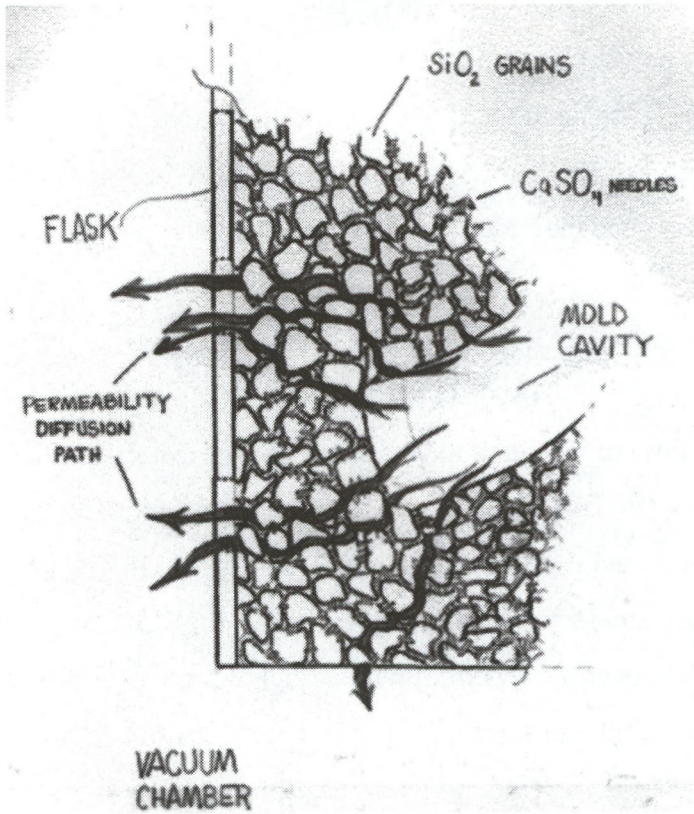


**Figure 1: Schematic diagram of silica and calcium sulfate structure in jewelry casting investment.**

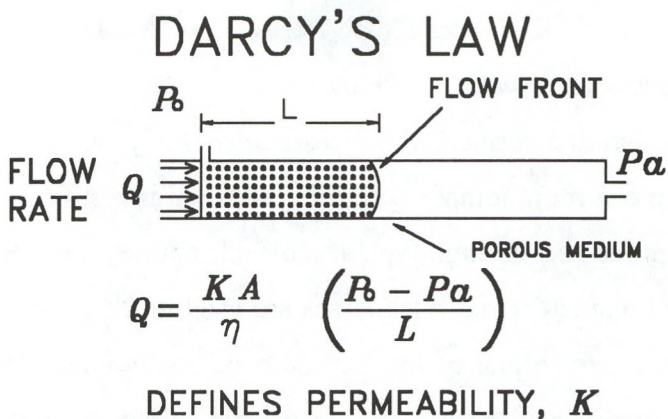
matrix of calcium sulfate needles. Figure 1 is a sketch of the proposed structure of jewelry casting investment. The structure suggests that permeability is a function of the characteristics of the calcium sulfate binder. The flow path for a gaseous fluid must lie within the calcium sulfate binder since individual grains of silica are not porous and cannot be penetrated.

### PERMEABILITY MEASUREMENTS

The flow of viscous fluids through porous materials is described by the empirical law of D'Arcy. D'Arcy observed flow rates and pressure drops that occurred in water flowing through a column of sand. Data was used to calculate the resistance of the sand to fluid movement. The principles have been extended to more complex fluid flow systems and are presented in an Internet tutorial by the University of Michigan.<sup>5</sup>

Permeability is determined by measuring the flow rate of a viscous fluid through a sample and the pressure drop that is required to achieve the observed flow. A graphical plot of flow versus pressure drop coupled with sample dimensions is used to calculate numerical values for permeability. Permeability is typically reported in units called "D'Arcys". Figure 2 is an example of the simple model that is usually used for permeability measurements.

Values for investment permeability are hard to find in the technical literature. Shell<sup>4</sup> et. al. describe a method used to measure permeability of dental investment at elevated temperatures. "Permeability" values were reported as flow rate through a specimen. Comparing the data reported in this investigation with values reported as D'Arcys is not possible.



|            |   |
|------------|---|
| K          | Permeability of the preform             |
| A          | Cross sectional area available for flow |
| $\nabla P$ | Pressure drop                           |
| $\eta$     | Fluid viscosity                         |
| $\phi$     | Porosity                                |
| L          | Length of the preform                   |

Figure 2: Schematic diagram of the flow model used for permeability determination.

## PERMEABILITY OF INVESTMENT CASTING MOLDS

Conversations with individuals who are involved with investment casting revealed that permeability measurements of jewelry investment are typically done at room temperature on cylindrical investment samples that have been processed through typical mold burnout cycles. Samples with standardized diameters and thicknesses are used in a device which applies elevated pressures to one of the flat sides of the sample. Pressure drop across the sample and corresponding gas flows are measured. Flow is very directional through the sample thickness. Values for permeability are determined from flow cross sectional area, flow rate, and pressure data. This investigation was undertaken to evaluate the permeability characteristics of typical jewelry investment molds at the elevated temperatures that are used when molds are cast.

Jewelry investment casting flask are cylindrical in shape. Test patterns with cylindrical shapes that are compatible with jewelry casting flasks and molds were developed so that experimental data could be obtained under conditions that were very similar to those used in standard investment casting operations.

The mold vacuum chamber of a bottom pour, pressure-over-vacuum, industrial casting machine was selected as the primary working tool for permeability studies. Many hours of casting operations indicated that this equipment was reliable, the pump-down rate of the vacuum chamber was rapid, and low, stable levels of vacuum could be consistently achieved. One modification was required to the equipment. Threaded studs were attached to the top cover plate of the vacuum chamber so molds could be clamped in place for the duration of an experimental run.

Permeability was measured with samples that were made in conventionally sized 4x8-inch jewelry investment casting flasks and commercial jewelry casting investment. Mold cavities were designed so that airflow conditions from an interior mold cavity to an external vacuum could be measured. Mold designs and measurement probe are described in Figures 3, 4, and 5. Details are as follows.

Two types of wax patterns were used for these experiments. One pattern was a flat disc approximately 1" inch thick and 2 3/4" inches in diameter. When invested in a mold, a cylindrical ring of investment approximately 5/8 inch thick was created between the cylindrical vertical wall of the mold cavity and the flask. Slotted windows with the same height as the thickness of the pattern were cut into the flask wall directly opposite the edge of the pattern. A bottom was welded onto the flask so that all flow through the flask had to exit from the mold through the slotted windows.

A second pattern that had the appearance cylindrical can was designed. The pattern was approximately 1 3/4" inches high and 1.7" in diameter. This pattern was also used with a totally enclosed flask that had slotted windows of the same height as the pattern in a direct flow path from the mold cavity to the external vacuum chamber.

This attempt to measure investment permeability with molds and test cavities that have circular or radial symmetry is based on the single critical assumption that no significant flow occurs through the top and bottom of mold cavities and all flow is through the edge of the cavity. The design features of the cavities used in experiments are as follows. The edge of the disc cavity had a surface area of 8.64 in<sup>2</sup> (55.73 cm<sup>2</sup>) and the

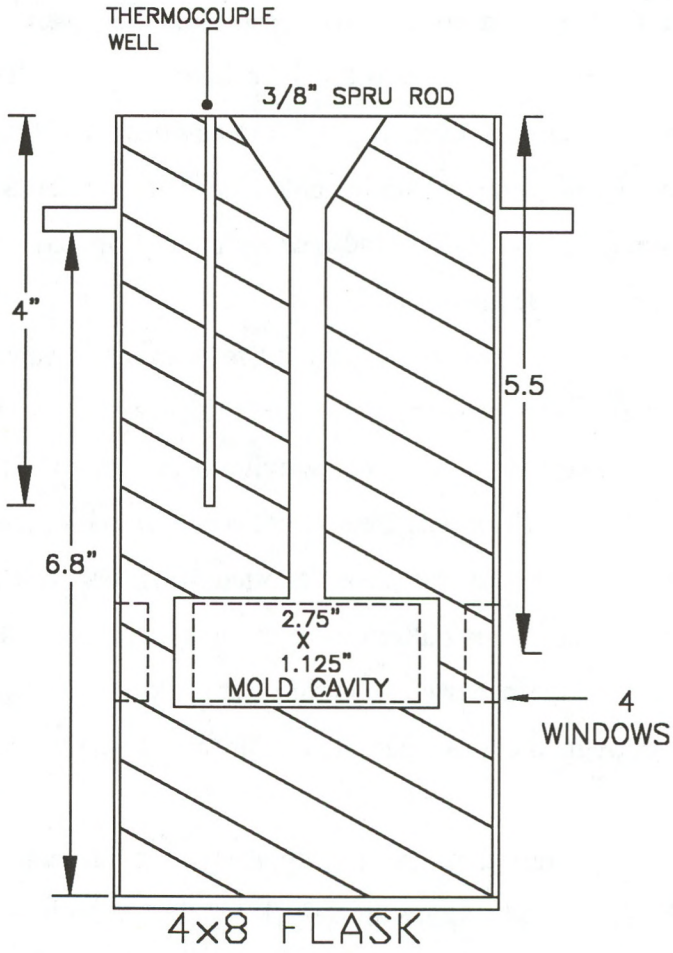


Figure 3: Mold cavity and flask design used for permeability determinations with "disc" patterns.



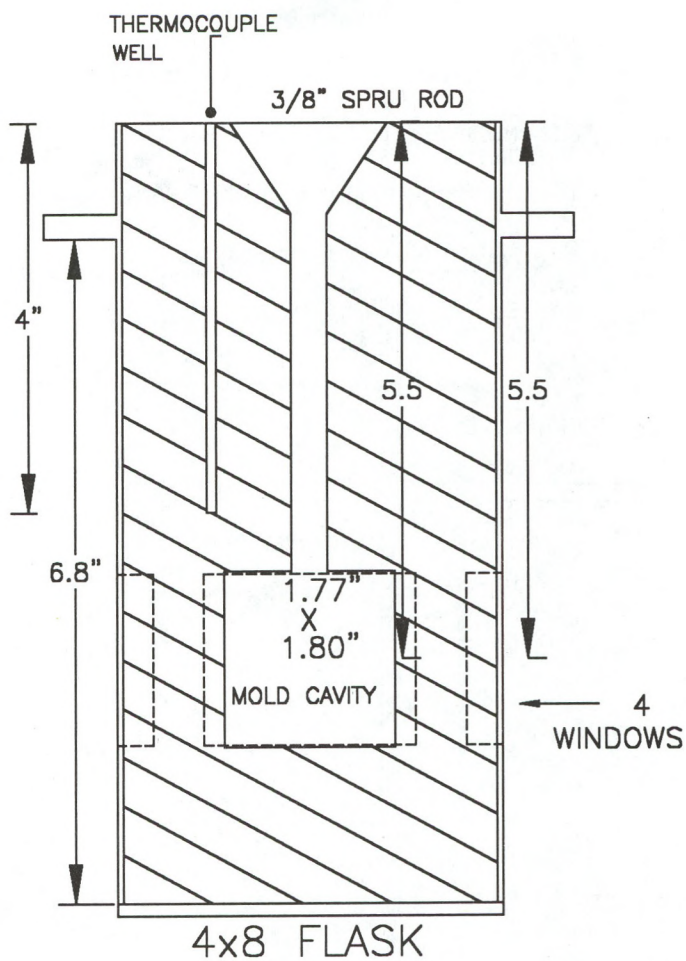


Figure 4: Mold cavity and flask design used for permeability determinations with "cylindrical" patterns.

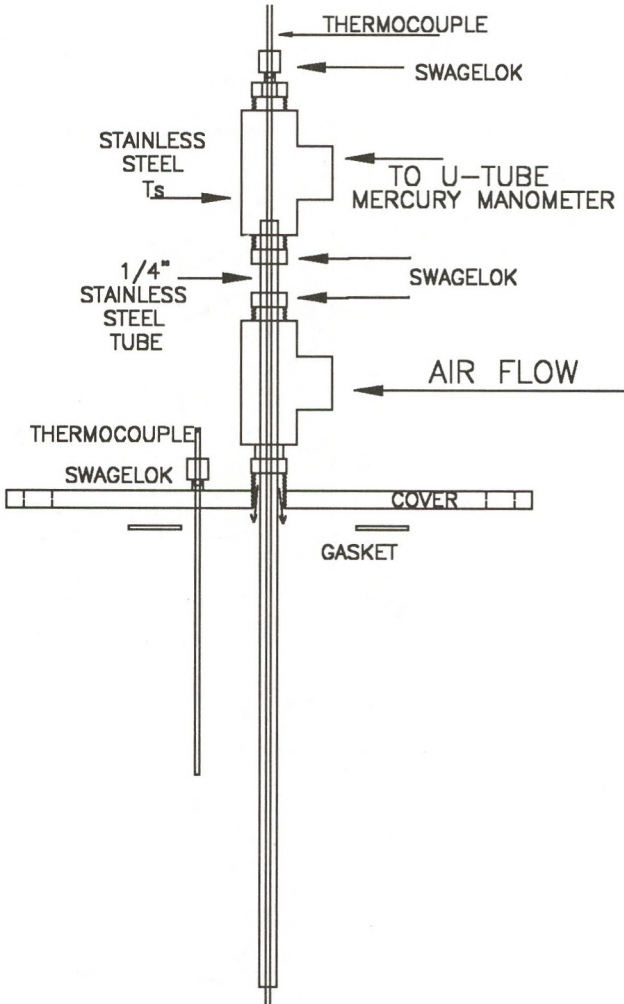


Figure 5: Detailed design of monitoring probe for pressure and temperature measurements required for permeability calculations.

surface area of the edge of the cylindrical cavity is  $9.35 \text{ in}^2$  ( $60.28 \text{ cm}^2$ ) in these experiments. The window in the flask wall used with disc patterns was  $10 \text{ in}^2$  ( $64.5 \text{ cm}^2$ ) and the window in the flask wall used with cylindrical patterns was  $17.5 \text{ in}^2$  ( $112.9 \text{ cm}^2$ ). These window areas indicate that flow from the plaster into the vacuum chamber at the mold surface should not have been restricted.

When used as patterns in an investment casting mold, these designs create a very simple sample for permeability measurements. In simple terms, the disc pattern creates a shell of investment with a wall thickness of 0.625 inches and the cylinder creates a shell of investment 1.115 inches thick. Once again, measured flow is assumed to travel through these shells in a radial direction into a vacuum chamber.

Using a sample cavity with radial or circular symmetry might appear to be the hard way to do permeability measurements, especially if measurements are usually done with flat samples of uniform cross section and thickness with fluids that move in one linear direction through the sample being tested. This is not really true. A simple equation to describe fluid flow from a cylindrical mold cavity can be found in heat transfer literature.

Schuhmann<sup>6</sup> presents an equation for heat flow through an insulated pipe. The flow of heat through an insulating layer is analogous to the flow of air through a porous medium. The heat loss from the surface of the pipe is:

$$q = - \frac{k 2\pi l \Delta t}{2.3 \log r_2/r_1} \quad (1)$$

Where  $q$  = rate of heat flow.

$k$  = thermal conductivity of insulation.

$l$  = pipe length.

$\Delta t$  = temperature difference between interior/exterior surfaces of insulation.

$r_2, r_1$  = outside and inside radius of insulation, respectively.

This equation can be rewritten as a solution to air flowing through a porous solid in the following manner.

$$Q = - \frac{K}{\eta} \frac{2 \pi l \Delta P}{2.3 \log r_2/r_1} \quad (2)$$

Where

$Q$  = rate of airflow.

$K$  = permeability.

$\eta$  = Viscosity of air.

$l$  = length or thickness of test pattern.

$\Delta P$  = Pressure drop across porous solid.

$r_2, r_1$  = Outside, inside radius of solid, respectively.

If flow rate  $Q$ , is plotted versus pressure drop,  $\Delta P$ , the slope of the plotted line,  $m$ , is equal to.....

$$m = \frac{\Delta Q}{\Delta P} = - \frac{K}{\eta} \frac{2 \pi l}{2.3 \log r_2/r_1} \quad (3)$$

Substituting appropriate values for the terms in this equation allows permeability,  $K$ , to be calculated. Values for the viscosity of air were taken from the Handbook of Chemistry and Physics<sup>7</sup>.

Pressure and temperature data from mold cavities was measured with a special probe described in Figure 5. The probe was screwed into the cap, which clamped the molds into the vacuum chamber. The main part of the probe was stainless steel tube that extended through the mold cap and into the mold cavity for pressure measurements. Cavity pressures were measured with a mercury U-tube manometer. A thermocouple extended through the pressure measuring tube into the mold cavity to measure the cavity temperature. A second thermocouple was located in the mold at a mid-radius location to monitor mold temperature.

Air that had passed through a ball flow meter was fed through the tee-fitting on the mold cap. Air entered the mold at the top of the sprue and was heated as it flowed down the sprue, into the mold cavity, through the mold, and out into the vacuum chamber. A complete diagram of the experimental set-up is presented in Figure 6.

## EXPERIMENTAL PROCEDURES

Patterns were invested in a commercial, gypsum bonded investment during normal mold production cycles, burned out according to a standard burnout cycle, and placed in the vacuum chamber of a commercial, vacuum assisted casting machine for final permeability measurements. The specially designed probe was placed in the center of the sprue post, locked into place and in this matter, the hot mold was sealed into the vacuum chamber of the casting machine.

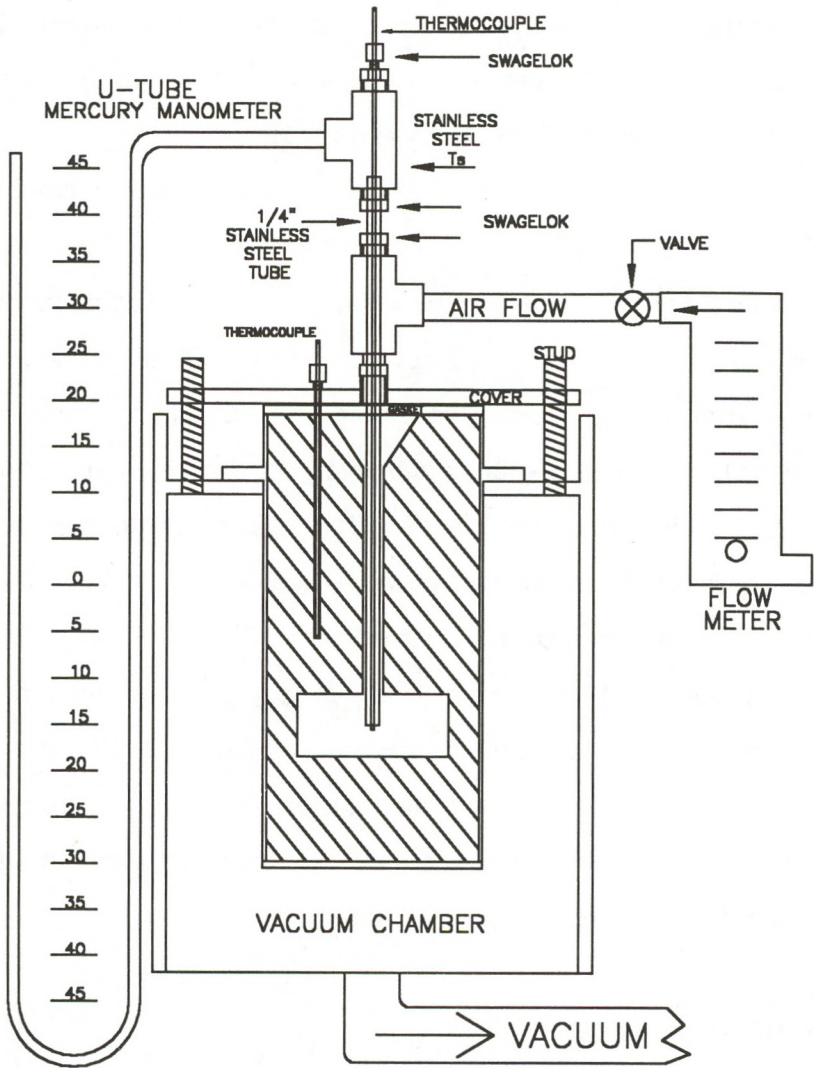


Figure 6: Schematic diagram of experimental set-up used for permeability measurements.

An experimental set-up was checked for indication of leaks at the start of each experimental run. The flask was set in position, manometer attachments were made and the mold cavity pumped down with no airflow allowed through it.

The time to reach a stable, reduced pressure in the mold cavity was used to evaluate tightness of the system. Vacuum chamber pressures were checked at the beginning, midpoint, and end of each experimental run. They were typically the same at each measurement time.

Mold temperatures were measured at a mid-radius location between the sprue post and the outside of the flask at positions that were remote from the mold cavity. Typically, mold temperatures were slightly higher than cavity temperatures because of the cooling effect of the airflow at the cavity location.

A ball valve was used to control the airflow. A typical experimental run involved the collection of data for air flow, mold cavity pressure, cavity temperature and mold temperature under conditions where air flow and cavity pressure appeared to reach stable, constant values.

## EXPERIMENTAL RESULTS

Figure 7 is a plot of flow versus pressure drop that was observed with disc and cylindrical mold cavities at mold temperatures over the range of approximately 1150 - 1300°F. Airflows in the range of 100 - 800 cc/min. were easily measured. Pressure drops were in the range of 15-70 cm Hg. The flow versus pressure data is linear when plotted and appears to fall into two distinct clusters. Slightly higher flow rates were observed with disc-shaped sample cavities.

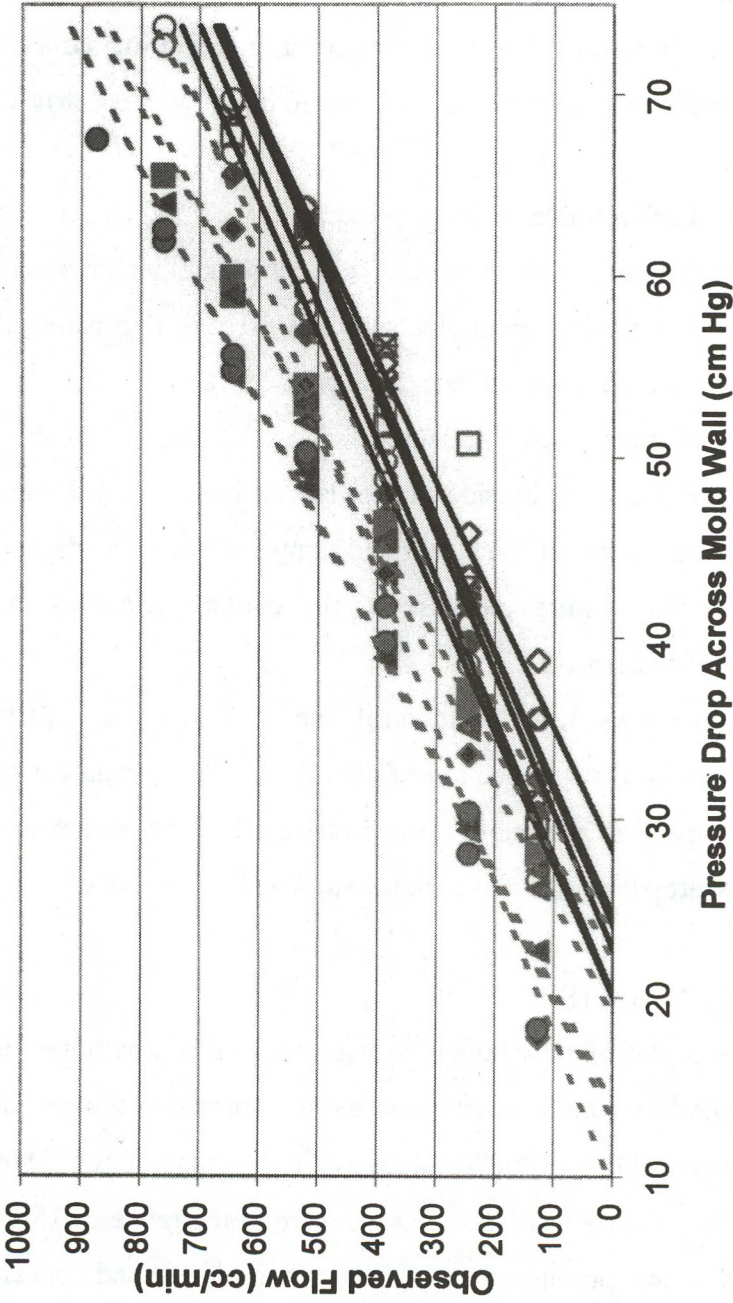


Figure 7: Flow versus pressure drop observations with "disc" cavities (dashed lines) and "cylindrical" cavities (solid lines) at 1100-1280 F during various permeability measurement trials.



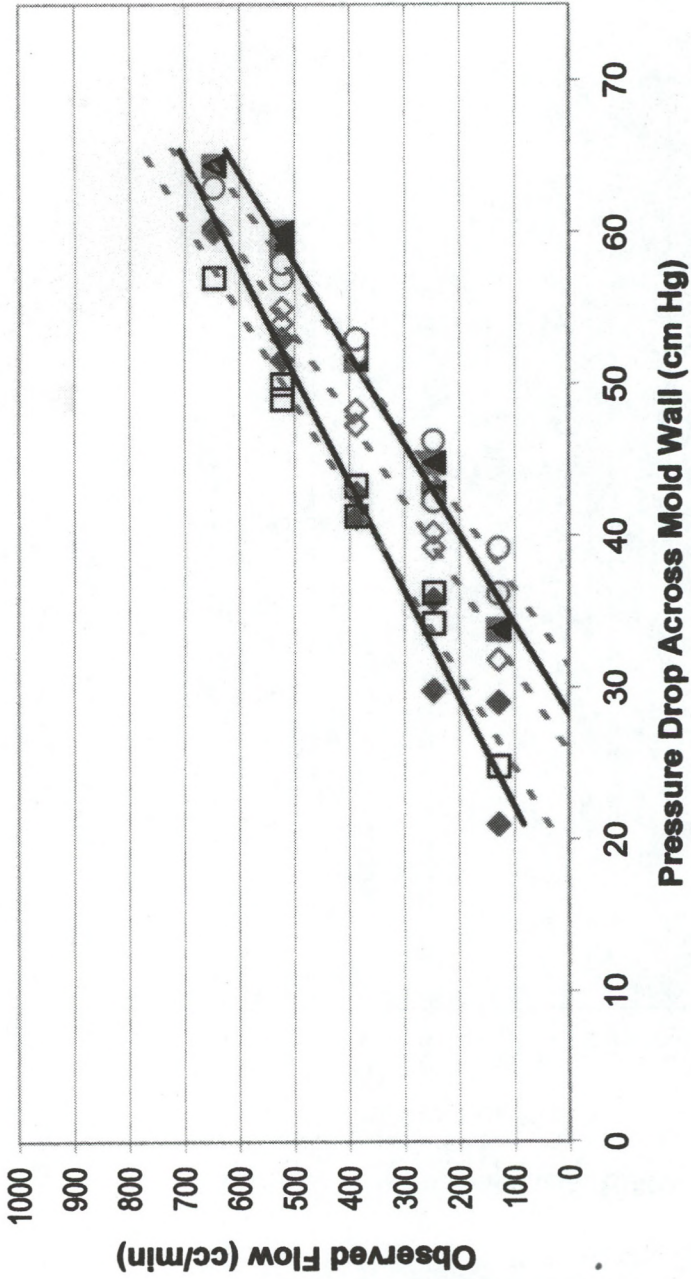


Figure 8: Flow versus pressure drop observations with "disc" cavities (dashed lines) and "cylindrical" cavities (solid lines) at 830-900 F during various permeability measurement trials.

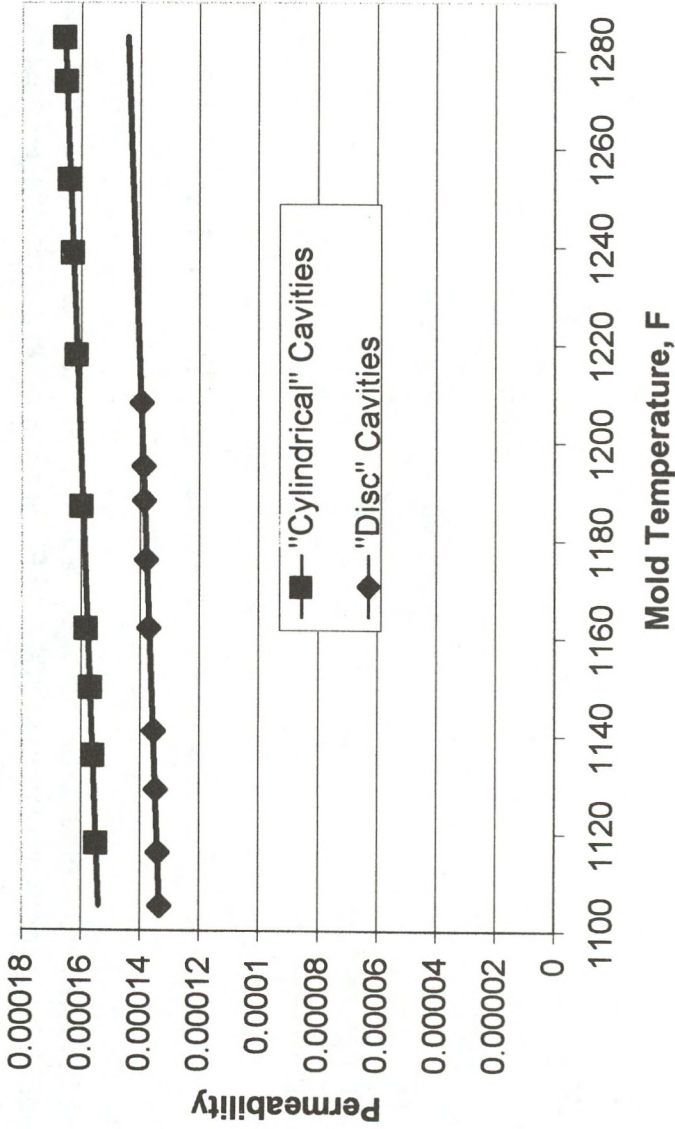


Figure 9: Permeability of gypsum bonded silica jewelry casting investment versus temperature as determined with "disc" and "cylindrical" cavities.

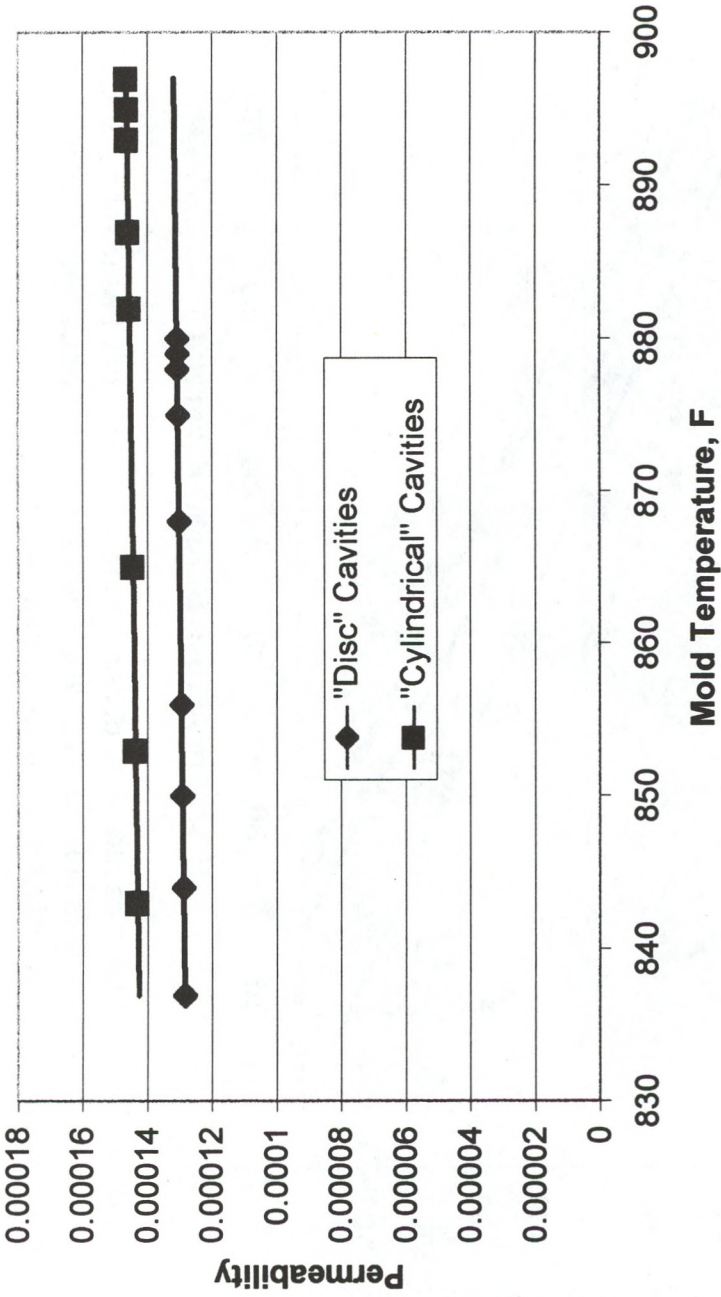


Figure 10: Permeability of gypsum bonded silica jewelry casting investment versus temperature as determined with "disc" and "cylindrical" cavities.

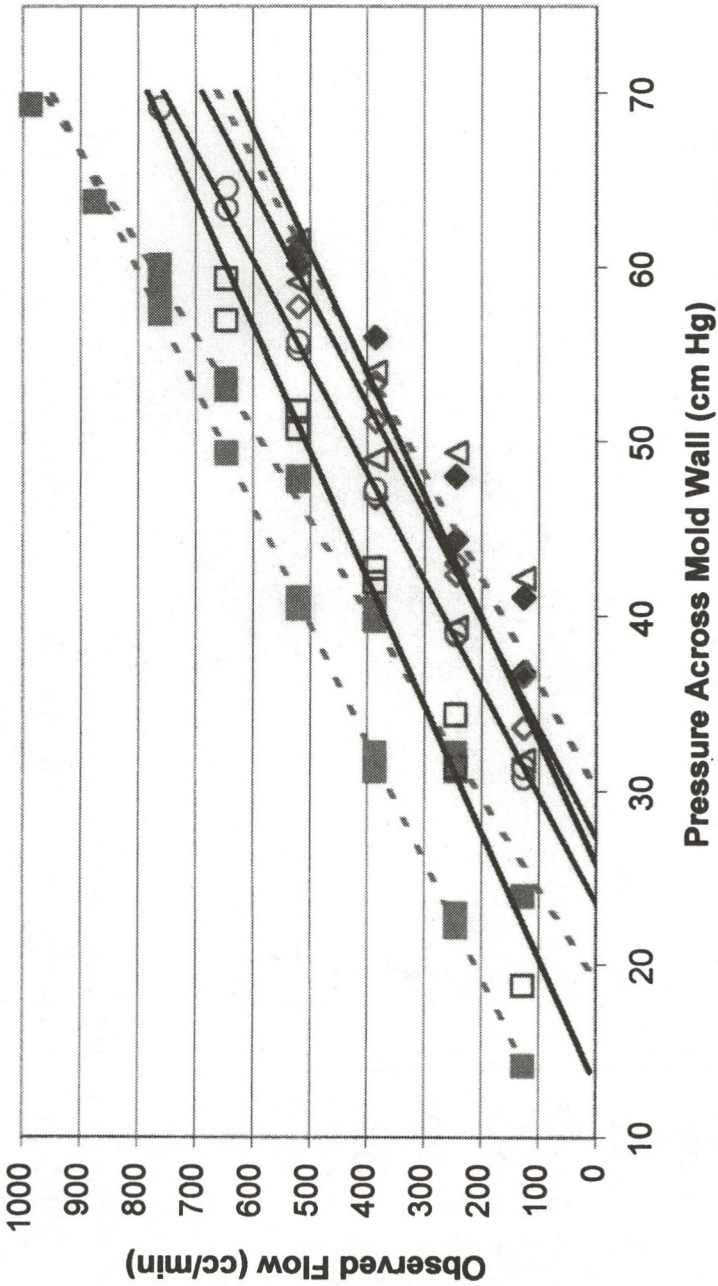


Figure 11: Flow versus pressure drop observations with "disc" cavities (dashed lines) and "cylindrical" cavities (solid lines) at 1100-1280 F during various permeability measurement trials with conventional perforated flasks.

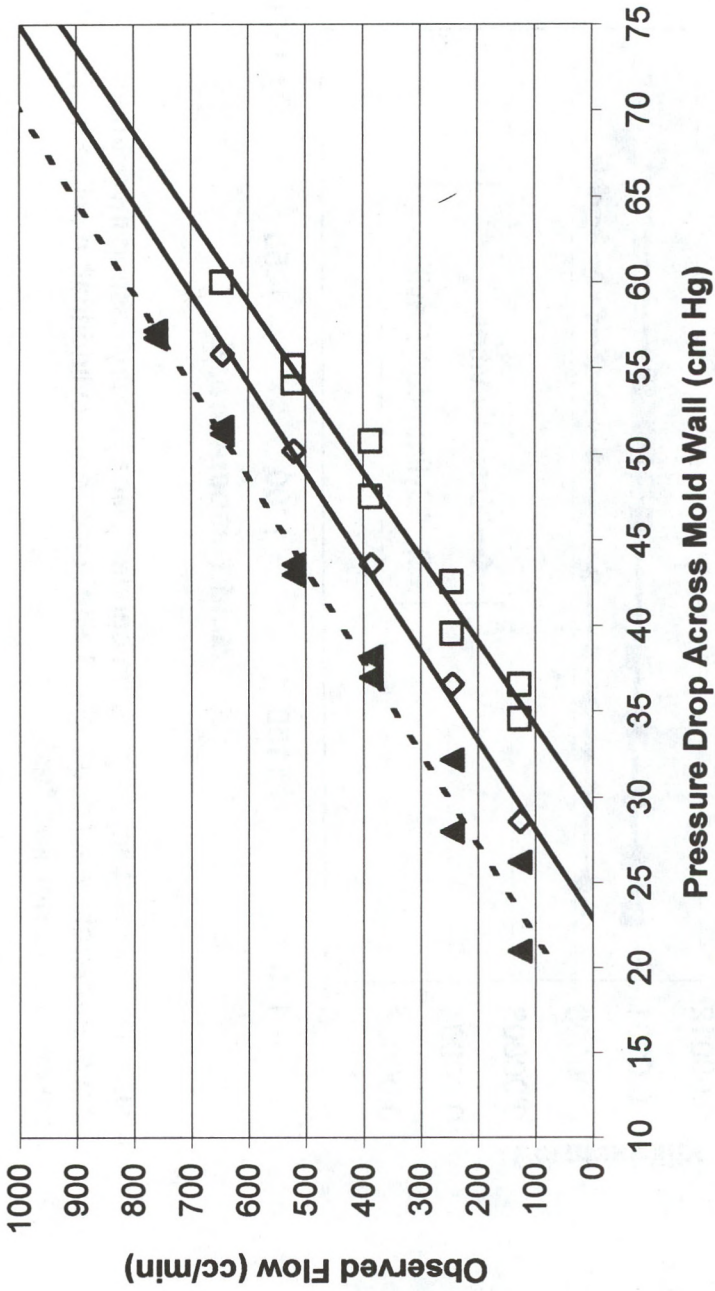


Figure 12: Flow versus pressure drop observations with "disc" cavities (dashed lines) and "cylindrical" cavities (solid lines) at 760-880 F during various permeability measurement trials with conventional perforated flasks.

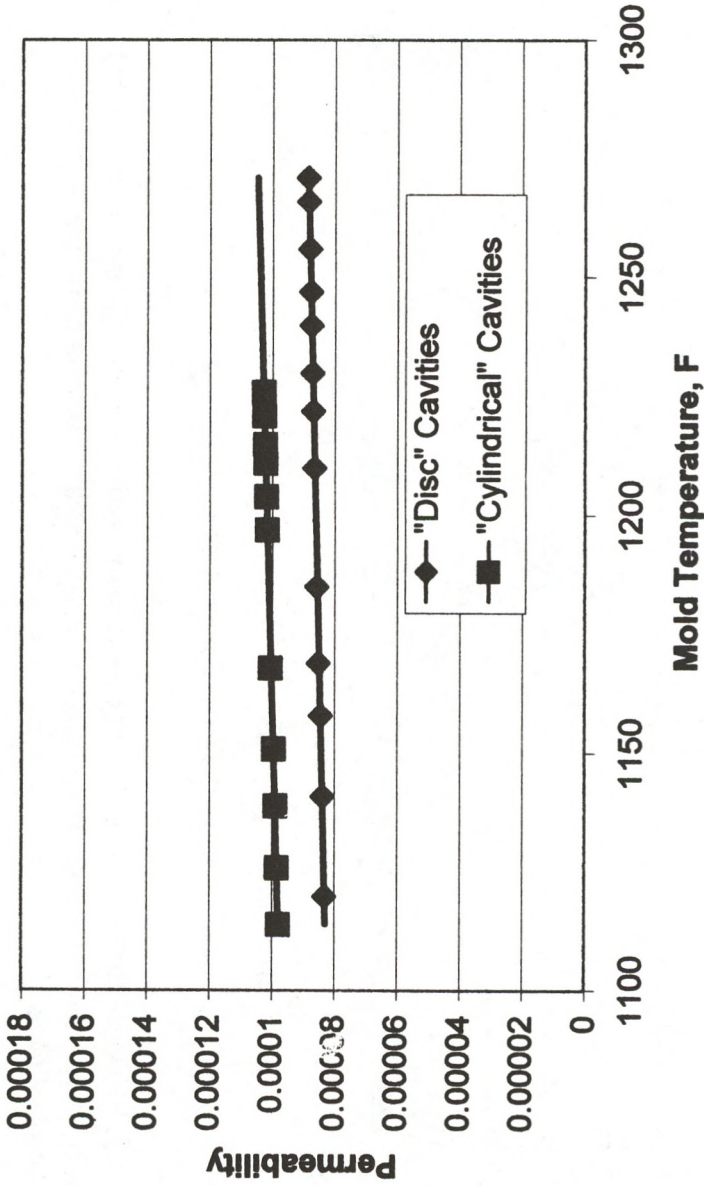


Figure 13: Permeability of gypsum bonded silica jewelry casting investment versus temperature as determined with "disc" and "cylindrical" cavities in a conventional perforated flask.

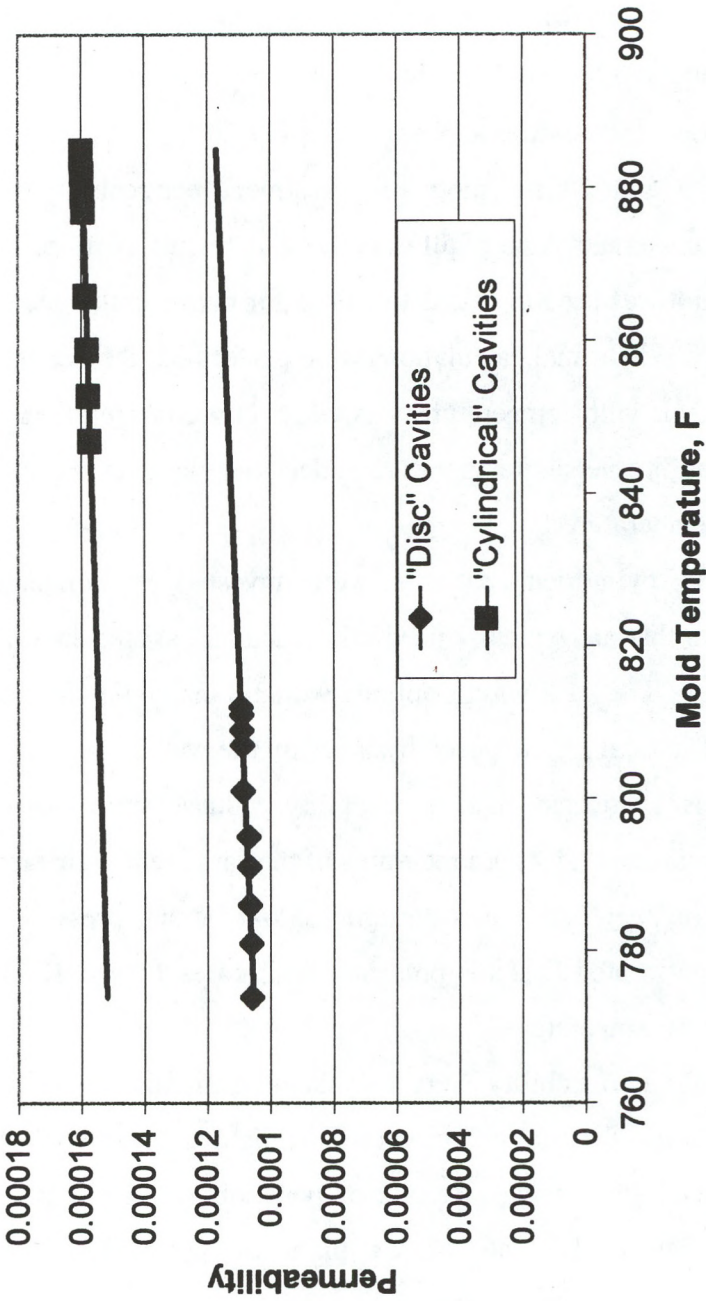


Figure 14: Permeability of gypsum bonded silica jewelry casting investment versus temperature as determined with "disc" and "cylindrical" cavities in a conventional perforated flask.

Figure 8 is a plot that is similar to Figure 7 for data collected in the temperature range of 770 - 900°F. The flow versus pressure drop for both disc and cylindrical test cavities appears to overlap.

Figures 9 and 10 are plots of investment permeability versus temperature. An average slope of all the flow vs. pressure plots described in Figures 7 and 8 was used to calculate values for permeability according to equation (3). When final calculations were performed, the variation of the viscosity of air with temperature was taken into consideration. The plots of permeability versus temperature reflect the slight changes in air viscosity with temperature.

Disc and cylindrical patterns were invested in conventional perforated flasks that are typically used with vacuum assisted investment casting machines. The flask was perforated with 3/8 inch holes and had an open bottom. The total area exposed by holes on the wall of the flask was 10.6 in<sup>2</sup>. It is suggested that permeability values determined with conventional perforated flasks are measures of the "apparent permeability" of both the investment and flask design. Flow versus pressure drop observed with perforated flasks is presented in Figures 11 and 12 at two different ranges of temperature.

Values for permeability were calculated from the slopes of the flow versus pressure drop graphs presented in Figures 11 and 12 by the methods described previously. Results of permeability calculations are presented in Figures 13 and 14 as plots of permeability versus temperature.

Finally, limited permeability measurements were performed on an experimental sample of investment supplied by a vendor. Flow versus



pressure drop and calculated values for investment permeability are presented in Figures 15 and 16, respectively.

## DISCUSSION:

Values for investment permeability measured in D'Arcy's at elevated temperatures are summarized in the following table.

**TABLE 1**  
**Measured permeability of gypsum bonded investment**  
**under different conditions, D'Arcys.**

|                                 | 800°F        | 1300°F           |
|---------------------------------|--------------|------------------|
| Disc w/Slot Flask               | 0.000128-131 | 0.000133-139     |
| Cylinder w/Slot Flask           | 0.000143-146 | 0.000154-166     |
| Disc w/Perforated Flask         | 0.000106-110 | 0.000083-88      |
| Cylinder w/Perforated Flask     | 0.000157-160 | 0.000097-0.00010 |
| Disc w/Slots, Experimental Inv. |              | 0.000144-156     |

Permeability values calculated with data from disc and cylindrical mold disagree by 12-15% within the same range of temperatures. Permeability values determined with cylindrical cavities are 12-15 percent higher than those calculated with cylindrical cavities. This suggests that the critical assumption of no significant airflow through the top and bottom of the cylindrical cavity is less valid than for the disc cavity. For a cavity of the same shape, temperature did not have a major effect on permeability. Permeability measured at approximately 1200°F was 4-13%

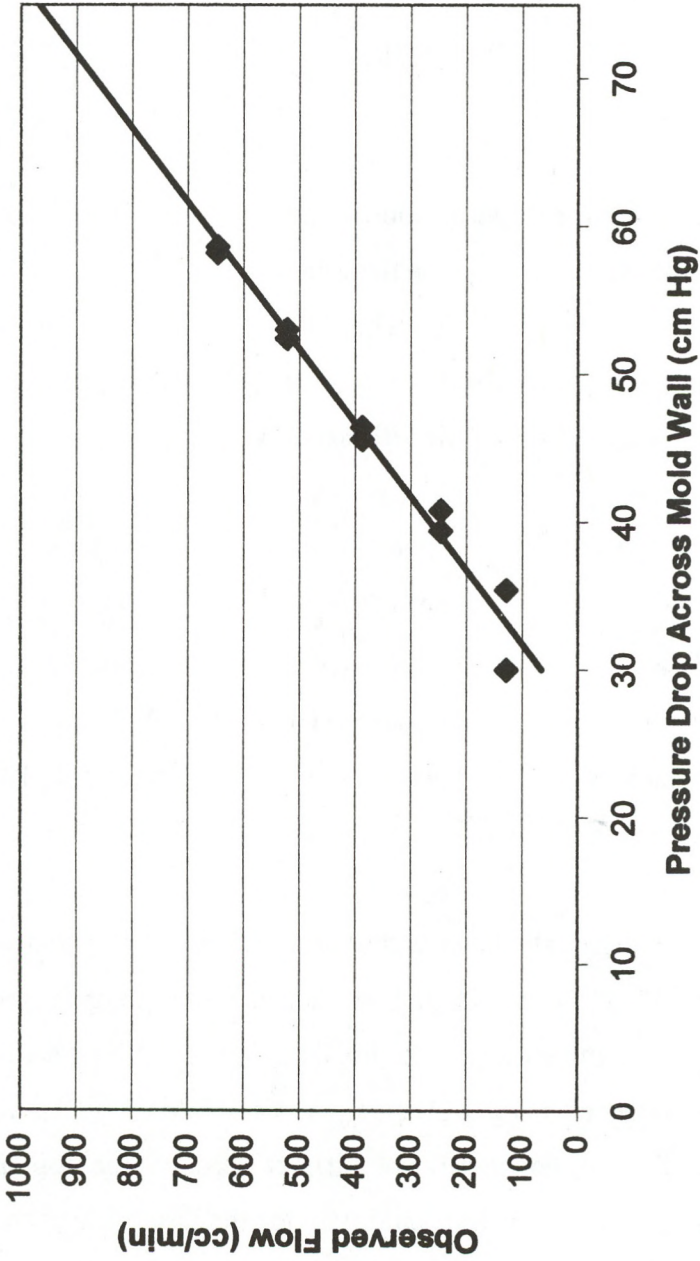


Figure 15: Flow versus pressure drop observations with a "disc" cavity at 1080-1280 F during permeability measurement on an experimental investment.

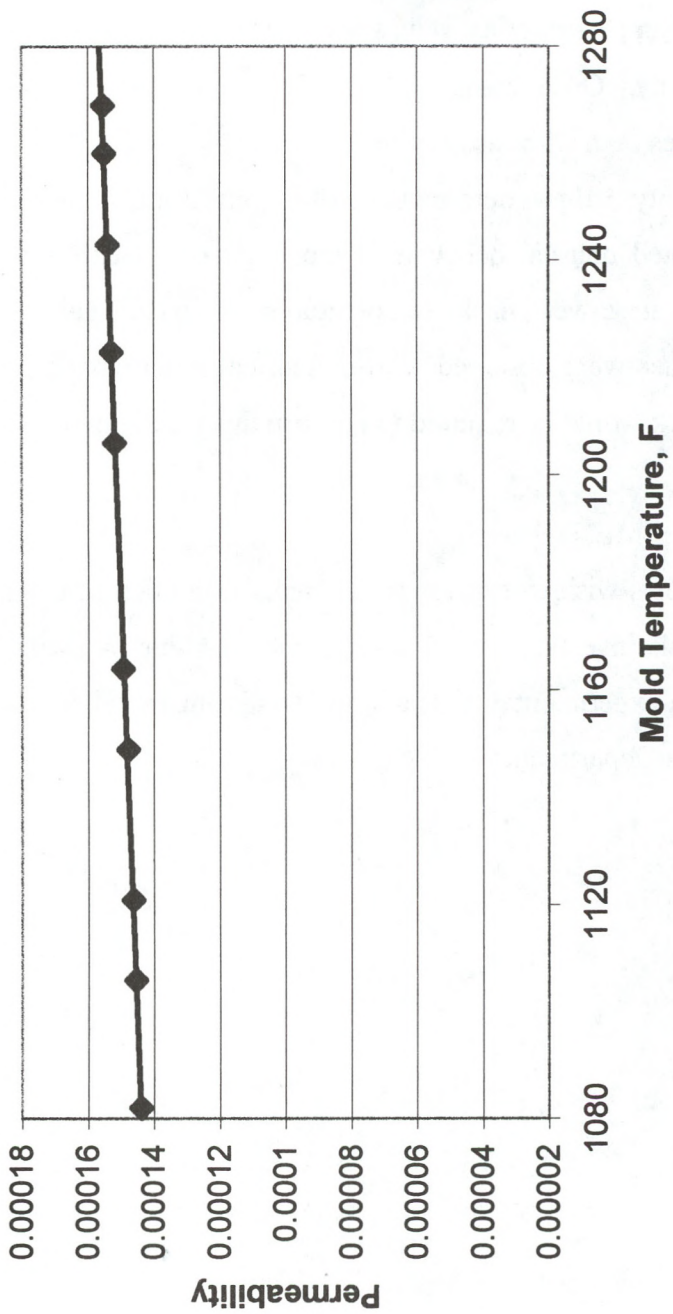


Figure 16: Permeability of an experimental gypsum bonded silica jewelry casting investment versus temperature as determined with a "disc" mold cavity.

percent greater than permeability values determined at 800°F for the same type of mold cavity. Once again, greater differences were observed with cylindrical cavities than with disc cavities.

Permeability values determined with conventional "perforated" flasks demonstrated unusual behavior in that higher permeability values were observed at lower flask temperatures. Once again, higher permeability values were observed with cylindrical mold cavities. More experimental work would be required to confirm this observation.

#### ACKNOWLEDGEMENTS

The author's wish to express their thanks to Stuller Settings, Inc., for supporting this investigation. Special thanks are due to Doug Leger for assisting with experimental trials and to Dennis Busby for allowing us to use his Casting Department.

## REFERENCES

1. Schwartz, Carl H.; Chemical and Physical Properties of Investment, Proceedings, Santa Fe Symposium on Jewelry Manufacturing Technology, 1987, page 99. D. Schneller, ed.
2. Kingery, W.D., Introduction to ceramics, J. Wiley & Sons, N.Y., 1960, pp. 55, 451.
3. Ott, Dieter; Properties and Testing of Investment, Proceedings, Santa Fe Symposium on Jewelry Manufacturing Technology, 1998, p. 47. D. Schneller, ed.
4. Shell, J.S., and Dortz, E.R. Journal of Dental Research, 1961, pp. 999 – 1003.
5. Intelligent Systems Lab, Michigan State University, 1997, [http://isl.cps.msu.edu/trp/rtn/modl\\_mes.ktml](http://isl.cps.msu.edu/trp/rtn/modl_mes.ktml).
6. Schuhmann, R., Metallurgical Engineering, Addison – Wesley Press, 1952, pp. 198-199.
7. Handbook of Chemistry and Physics, 67<sup>th</sup> Edition, CRC Press, 1986-87, pp. F-11, 12.

